Surface Strain Improves Molecular Adsorption but Hampers Dissociation for N_2 on the Fe/W(110) Surface

I. Goikoetxea,[1,2,*] J. I. Juaristi,[3,2,4,†] R. Díez Muiño,[2,4,‡] and M. Alducin[2,4,§]

[1]*Humboldt Universität zu Berlin, Institut für Chemie, Unter den Linden 6, D-10009 Berlin, Germany*

[2]*Centro de Física de Materiales CFM/MPC (CSIC-UPV/EHU), Paseo Manuel de Lardizabal 5, 20018 Donostia-San Sebastián, Spain*

[3]*Departamento de Física de Materiales, Facultad de Químicas (UPV/EHU), Apartado 1072, 20080 Donostia-San Sebastián, Spain*

[4]*Donostia International Physics Center (DIPC), Paseo Manuel de Lardizabal 4, 20018 Donostia-San Sebastián, Spain*

(Received 4 June 2014; published 4 August 2014)

We compare the adsorption dynamics of N_2 on the unstrained Fe(110) and on a 10% expanded Fe monolayer grown on W(110) by performing classical molecular dynamics simulations that use potential energy surfaces calculated with density functional theory. Our results allow us to understand why, experimentally, the molecular adsorption of N_2 is observed on the strained layer but not on Fe(110). Surprisingly, we also find that while surface strain favors the molecular adsorption of N_2 it seems, on the contrary, to impede the dissociative adsorption. This result contrasts with previous examples for which strain is found to modify equally the energetics of chemisorption and dissociation.

DOI: 10.1103/PhysRevLett.113.066103 PACS numbers: 68.43.−h, 34.35.+a, 82.20.Kh, 82.65.+r

The adsorption of nitrogen on iron surfaces is the standard textbook example when linking basic surface science and industrial heterogeneous catalysis [1]. N_2 adsorption and dissociation is the rate limiting step in ammonia synthesis and iron-based compounds are the preferred solid catalyzers for such a process. It is not a surprise then that extensive research has been devoted to understand and ameliorate the chemistry between N_2 and Fe surfaces [2–10]. Chemical properties can be locally altered by several elements, including defects, steps, and/or other adsorbed species. Local strain at the surface has been also shown to change surface reactivity in a significant way [11,12]. However, tuning the adsorption properties in the extended surface is much more involved. A clever way to do so is the pseudomorphic growth of ultrathin metallic films on top of substrates with different lattice constants. The electronic properties of the stretched (compressed) surface can be substantially modified giving rise to profound changes in the adsorption energetics between strained and unstrained surfaces [13–20]. Hitherto, all the studied systems show that the overall adsorption properties are equally altered, i.e., that the atomic, molecular, and dissociative adsorption are either all improved or all reduced.

In the particular case of N_2, it has been experimentally shown that the growth of Fe layers on W(110) strongly enhances the adsorption and dissociation of N_2 as compared with the otherwise fairly unreactive Fe(110) surface [6]. These observations agree with the above mentioned existing understanding of how surface strain affects the overall adsorption properties. However, we show here by means of molecular dynamics simulations that while surface strain favors molecular adsorption due to a uniform reduction of the energy barriers accessing the wells, its effect on the energetics of the dissociation process is surprisingly the opposite and, therefore, the observed atomic N cannot be directly attributed to surface strain in this case. We actually find that the minimum energy barrier to dissociation found in Fe(110) increases by about 500 meV in Fe/W(110). Interestingly, this energy upshift is not uniformly reproduced in all the configurational space leading to dissociation and the result is a drastic change on the reaction path to N_2 dissociation. In spite of it, our dynamics simulations show that the efficiency for N_2 dissociation on the heteroepitaxial strained surface is reduced by a factor 1.5–2 that highly contrasts with the general improvement achieved for molecular adsorption.

The interaction of N_2 with the Fe/W(110) surface is described within the adiabatic and the frozen surface approximations by a six-dimensional (6D) potential energy surface (PES) that depends on the positions of the two N atoms. The continuous 6D PES is obtained by applying the corrugation reduction procedure [21] to interpolate a set of 20801 energy values. The latter are calculated for suitably selected positions of the N atoms with spin-polarized density functional theory (DFT) and the revised Perdew-Burke-Ernzerhof (RPBE) exchange-correlation functional [22] using the VASP code [23,24]. The pseudomorphically grown Fe/W(110) surface [25] is modeled by a periodic supercell that consists of six layers of W with a nominal interlayer distance $d = 2.24$ Å, one overlayer of Fe, and 15 layers of vacuum. A (2×2) surface unit cell avoids spurious interactions between the N_2 periodic images. The relaxed Fe/W(110) surface structure is calculated by keeping fixed the central W layer. After relaxation the distance between the Fe and the topmost W layer is 1.97 Å, which represents a contraction of around 12% with respect to the nominal value d. Additionally, the distance between the first and second W layers is increased around 1%. These

results are in nice agreement with previous calculations [26–28] and experiments [29]. Results presented for the N_2/Fe(110) system have been calculated with an improved version of the 6D PES used in [30] that incorporates 671 new DFT energy data to equal the *ab initio* grid used for the N_2/Fe/W(110) PES. We note, however, that the results from the dynamics simulations are almost unchanged [31].

Starting with the molecular adsorption process on Fe/W(110), we find the same two adsorption configurations that were observed on Fe(110) [30]. In both surfaces the deepest energy well corresponds to the configuration in which the N_2 center of mass is over a hollow site with the molecular axis oriented parallel to the surface along the $[1\bar{1}0]$ direction. The second adsorption well is found for the molecule standing upright atop a Fe surface atom. These adsorption states will be denoted as hollow-parallel and top-vertical, respectively, in the following. Comparing state-to-state the adsorption properties of N_2 between the two surfaces (Fig. 1), there are no significant differences between the N_2 internuclear distance r and position Z of the center of mass from the surface at the minimum. In contrast, the change in the adsorption energies E_{ads} is quite significant, since the depth of the adsorption wells is more than 150 meV larger in Fe/W(110).

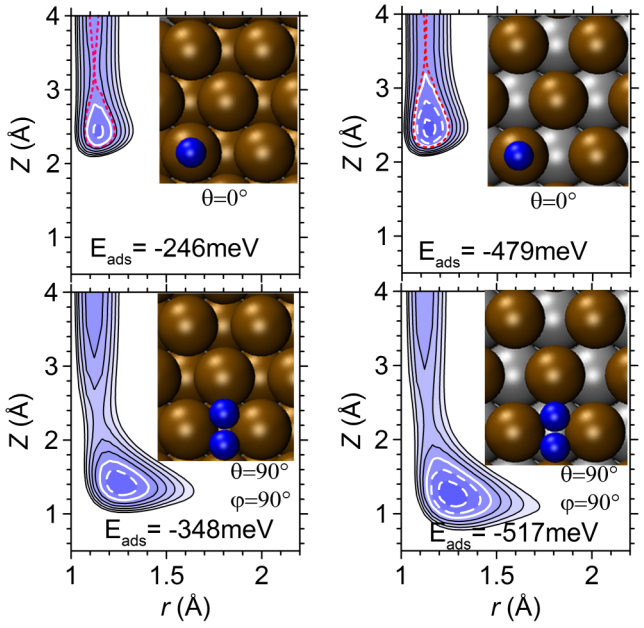

FIG. 1 (color online). Contour plots of the potential energy $E(r, Z)$ for the two molecular adsorption configurations found on Fe(110) (left panels) and Fe/W(110) (right panels). Black solid (white dashed) contour lines, separated by 0.2 eV, indicate positive (negative) potential energy values. White solid lines show the zero potential energy. The energy barrier of 50 meV (130 meV) to access the top-vertical well on Fe/W(110) [Fe(110)] is plotted with a red dotted contour line. The adsorption energy E_{ads} is obtained by interpolating the DFT energy grid for each configuration.

The adsorption of N_2 on Fe(110) and on Fe/W(110) for defined incidence energy E_i and normal incidence is simulated by classical dynamics calculations carried out with the adiabatic 6D PES and neglecting the N_2 zero point energy. Energy exchange between the molecule and the lattice is included in the equations of motion by means of the generalized Langevin oscillator model that allows us to perform calculations at a fixed surface temperature T_s [32,33]. For each E_i a conventional Monte Carlo procedure is used to sample the initial N_2 orientation and position over the (2×2) surface unit cell. All trajectories start with the N_2 molecule at its calculated equilibrium bond length of 1.11 Å and its center of mass at $Z = 6$ Å from the surface, where the potential energy is zero. In the simulations a molecule is considered dissociated when the two N atoms separate from each other beyond 2.22 Å with positive radial velocity and molecularly adsorbed when it has neither dissociated nor reflected after 30 ps and its total energy (kinetic plus potential) is negative.

The results for the molecular adsorption probabilities calculated from 5000 trajectories are shown in Fig. 2 for a surface temperature $T_s = 80$ K. In all cases, the probabilities initially increase with E_i due to the existence of energy barriers in accessing the wells and, next, decrease when E_i becomes too large to efficiently dissipate into the surface the excess kinetic energy that impedes the molecule to accommodate on the adsorption well. Common to both surfaces, we observe (left panel) that N_2 adsorption at low energies is dominated by the top-vertical well and not by the energetically favorable hollow-parallel well. This is a consequence of the different energy barriers that exist at the entrance of each adsorption site as it is discussed below. We also observe that the adsorption probability on the top-vertical state increases by at least a factor of 2 in the open

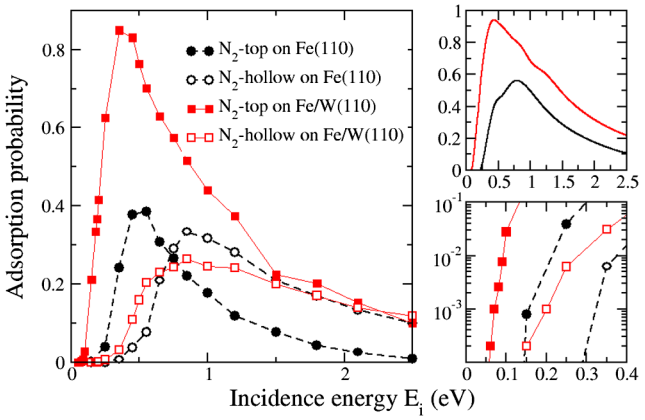

FIG. 2 (color online). All panels: Molecular adsorption probability of N_2 on Fe/W(110) (in red) and on Fe(110) (in black) as a function of the incident energy, for normal incidence and $T_s = 80$ K. Left- and right-bottom panels: Adsorption probability on the top-vertical (close symbols) and on the hollow-parallel (open symbols) wells. Right-top panel: Total molecular adsorption probability.

Fe/W(110), while adsorption on the hollow-parallel well is less modified. The final result is that the overall N_2 adsorption, plotted in the right-top panel of Fig. 2, is significantly enhanced on the strained Fe overlayer for all the E_i considered here.

The adsorption properties at low E_i deserve particular attention. As shown in the zoom-in plot of Fig. 2 (right-bottom panel), adsorption on Fe/W(110) requires a minimum E_i of ~50 meV that corresponds to the minimum barrier to access the top-vertical well (red contour line in Fig. 1), while a larger E_i of ~150 meV is necessary for adsorption on the hollow-parallel well. On Fe(110) the corresponding barriers to access each well increase by about 100 meV and, as a consequence, a minimum E_i of ~150 and ~250 meV are necessary in this case to observe adsorption on the top-vertical and on the hollow-parallel wells, respectively. These results are consistent with published experiments showing that at low surface temperatures thermally deposited N_2 adsorbs on the strained Fe/W(110) surface but not on Fe(110) [6]. Furthermore, our dynamics results explain why only the top-vertical state is identified from the angle-resolved ultraviolet photoemission spectra (ARUPS). Still, for the experimental conditions of [6] in which N_2 is thermally deposited at $T_s = 80$ K, one may argue that 50 meV is a too high energy barrier that may prevent N_2 adsorption. In this respect, it has been shown that despite the RPBE functional improves the calculated adsorption energies of molecules such as N_2 and O_2 in transition metal surfaces [22], it usually provides too high energy barriers at the entrance channel [34–38]. For this reason, we have also computed the potential energy of the top-vertical configuration as a function of the distance to the surface using the less repulsive PW91 functional [39]. While adsorption on Fe(110) was shown to remain activated also in this case [30], it would be nonactivated on Fe/W(110) in view of the barrierless $E(Z)$ curve we obtain. Thus, in agreement with experiments [6], this would imply an efficient adsorption of N_2 at the top-vertical well on Fe/W(110) and the lack of adsorption on Fe(110).

At variance with our findings for molecular adsorption, the inertness of Fe(110) towards N_2 dissociation, which is characterized by a dissociation probability smaller at least than 10^{-5} for $E_i < 1.5$ eV [30], is not reversed on Fe/W(110). This is precisely one of the conclusions extracted after running classical dynamics calculations under normal incidence and various E_i. As seen in Fig. 3(a), on Fe/W(110) the dissociation process remains activated and the dissociation probability values obtained from 50 000 trajectories are clearly smaller on this surface than on Fe(110).

What we also consider remarkable is that surface strain leads to a complete change of the minimum energy reaction path to dissociation. This can be observed in the snapshots of Fig. 3(b) that show the position of the center of mass of

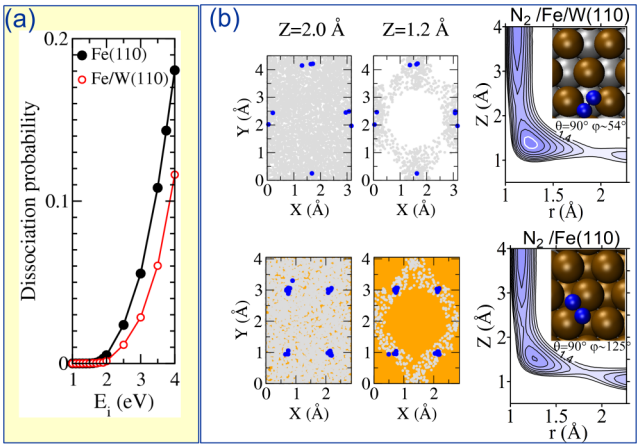

FIG. 3 (color online). (a) Dissociation probability of N_2 on Fe(110) (black circles) and on Fe/W(110) (red open circles). (b) Position of the N_2 center of mass over the surface unit cell when first reaching the distance $Z = 2.0$ and 1.2 Å: dissociating N_2 in blue and reflecting N_2 in gray. Upper (lower) panels show the results for Fe/W(110) [Fe(110)]. Simulations performed for $E_i = 1.7$ eV. The contour plot of the DFT configuration with the minimum energy to dissociation (depicted in the inset) is shown for each surface at the right of the snapshots. Contour lines as in Fig. 1.

the dissociating molecules over the surface unit cell in their approach to the surface. It is clear that the dissociating molecules concentrate about bridge position on Fe(110) (lower panels), whereas they do about the hollow site on Fe/W(110) (upper panels). This is a consequence of the nonuniform changes that the heteroepitaxial surface strain is causing in the configurational space leading to dissociation. Thus, we first observe that the minimum energy barrier of about 1.1 eV that was found in Fe(110) for the configuration over the bridge depicted in Fig. 3(b) lower inset increases to ~1.6 eV in Fe/W(110). In contrast, the minimum energy barrier for the configuration over hollow (Fig. 3, upper inset) slightly decreases from ~1.3 eV in Fe(110) to ~1.25 eV in Fe/W(110). Changes in the minimum energy path for H_2 dissociation have been recently found between the pseudomorphically grown Pd/Ru(0001) and the unstrained Pd(111) [17,18], also with the help of classical dynamics simulations. In this case, the reason is the nonuniform, though, in contrast to here, general upshift of the energy barriers on the strained Pd/Ru(0001).

The atomic N observed on Fe/W(110) after thermal deposition of N_2 at $T_s = 80$ K [6] contrasts with the high energy barrier of ~1.25 eV found here. Remarkably, the DFT energy barrier of ~1.1 eV for N_2 dissociation on Fe(110) [8,9,30] is also much larger than the experimental value of 0.27 eV [2]. This large mismatch found on both surfaces can hardly be attributed to the inherent limitations of DFT. In particular, we have verified that using the PW91 functional the minimum barrier is still ~0.6 eV on

Fe/W(110) and slightly smaller on Fe(110). Hence, there should be other reasons for such a discrepancy. Regarding our theoretical approximations, the use of classical mechanics is here well justified. The mass of N was shown to be large enough to neglect quantum tunneling effects in the dissociation of N_2 on stepped Ru(0001), a system with a dissociation barrier similar to ours [40]. An additional approximation consists in neglecting the modifications of the PES due to surface atoms motion. However, the mean surface atoms displacement caused by their thermal motion at 80 K is below 0.1 Å and implies a very minor effect in the barrier height. More pronounced can be the surface atoms displacement induced by their interaction with N_2. Thus, we have recalculated the dissociation energy barriers on both surfaces by allowing relaxation of the first two surface layers, but the barrier to dissociation on Fe/W(110) is still ~1 eV. Given that, on the one hand, the above analysis points to the robustness of the theoretical energy barriers that are similarly high on both surfaces and that, on the other hand, N_2 is efficiently adsorbed on Fe/W(110) but not on Fe(110), we suggest that the N observed on Fe/W(110) may be due to dissociation at steps or defects of the previously adsorbed N_2. Another possible scenario to consider would be if the eventual modification of the potential energy landscape in the surrounding of an already adsorbed molecular species might facilitate dissociation. All in all, the prevalent conclusion is that dissociation is not *directly* favored by surface strain. The fact of atomic N being measured on Fe/W(110) and not on Fe(110) suggests that dissociation may require previous adsorption of molecular N_2, efficient on the strained surface only.

Next, we try to rationalize the opposite effects that the strained Fe/W(110) surface has on the molecular and the dissociative adsorption. Starting with the molecular adsorption, a first detailed inspection of the orbital-and site-projected density of states (PDOS) of the whole N_2-metal system at the adsorption configurations shows that the adsorption properties are determined mainly by the interaction of the π_g^* state of N_2 with the *d*-band states localized at the surface topmost layer, since the hybridized σ_{p_z} and π_u are completely filled and only the first-layer-PDOS is clearly perturbed upon adsorption. As observed from the π_g^*-PDOS curves of Fig. 4, the occupation of the hybridized π_g^* states for each adsorption configuration are very similar in both surfaces (similar area below the cyan and brown curves for energies below the Fermi energy E_F). However, the filling process would be energetically more favorable for the strained surface because the unperturbed π_g^* (green lines) are energetically closer to E_F in Fe/W(110) than in Fe(110) due to the lower work function of the former. The latter would explain the deeper adsorption wells and the concomitant reduction of the energy barrier in accessing each well on Fe/W(110). Such a reduction seems to be a common feature of the N_2/Fe/W(110) PES at *Z* distances above 1.5–2 Å and, hence, of the configurations leading to

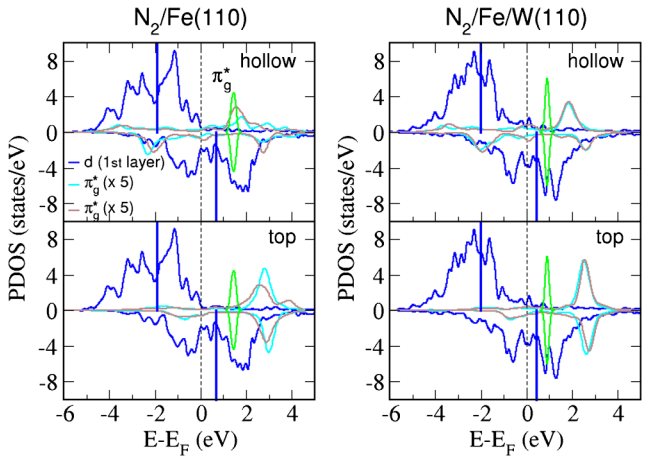

FIG. 4 (color online). Orbital- and site-PDOS resolved in spin-up (positive values) and spin-down (negative values) electrons. Dark blue curves represent the *d*- and first-layer-PDOS of the bare Fe(110) (left panels) and Fe/W(110) (right panels) surfaces. For completeness, the corresponding *d*-band centers ε_d are marked by dark-blue vertical lines. The π_g^*-PDOS (cyan and brown curves) are multiplied by a factor of 5. The (four degenerated) π_g^* levels of the noninteracting N_2 are shown by green lines.

dissociation too. In this case, however, the differences in the N adsorption properties between both surfaces are also relevant to understand the unexpected increase of the energy barrier to dissociation, as discussed next.

N_2 dissociation will occur when the *individual* N-surface atoms' attraction becomes greater than the strong N-N interaction. Schematically, dissociation along the bridge configuration, depicted in Fig. 3(b) lower inset, proceeds through the attraction of each N atom towards its nearest hollow site. Due to the large (10%) lattice expansion of the Fe monolayer on W(110) the minimum energy position of the N atom at the hollow site is ~0.2 Å closer to the surface on Fe/W(110) than on Fe(110). This makes the N atom feel a stronger repulsion with the second-layer atom beneath. As a result the overall N-surface interaction is about 200 meV less attractive on Fe/W(110) than on Fe(110) and there is a subsequent increase of the energy barrier along this dissociation path. In contrast, the N-surface atoms interaction at the bridge site, which is the relevant position for dissociation along the hollow configuration [upper inset in Fig. 3(b)], is similarly attractive on both surfaces and, hence, produces similar energy barriers. Increases of the barrier heights in other cases have been successfully explained by analogous arguments [15,41–43].

In summary, our comparative study on the adsorption dynamics of N_2 on the unstrained Fe(110) and on the strained Fe/W(110) surfaces explains the experimental observations of Homann *et al.* [6] showing that the inertness of Fe(110) towards N_2 adsorption disappears on Fe/W(110). In agreement with the reported ARUPS spectra, we also illustrate why N_2 adsorbs vertical to the

surface though the hollow-parallel adsorption well is energetically more favorable. Remarkably, we also demonstrate that the atomic N observed on Fe/W(110) in those experiments cannot be the result of surface strain as originally thought because, in fact, there is a notable increase of the minimum energy barrier to dissociation in the strained surface. The unexpected observation of a combined molecular adsorption improvement and dissociative adsorption reduction highly contrast with the common notion that associated surface strain with an overall increase or reduction of all kinds of adsorption events. We attribute the present unusual behavior to the excessive stretching of the Fe monolayer that hampers the efficiency of the N-Fe interaction in triggering dissociation. Probably, our finding is not specific of N_2 on Fe/W(110) as the central condition of a large tensile stretching can be achieved with many heteroepitaxial surfaces. In this respect, our work opens a new perspective on the role of surface strain to control the adsorption properties on surfaces.

This work was supported in part by the Basque Departamento de Educación, Universidades e Investigación, the University of the Basque Country UPV/EHU (Grant No. IT-756-13) and the Spanish Ministerio de Ciencia e Innovación (Grant No. FIS2010-19609-C02-02). Computational resources were provided by the DIPC computing center.

*itziar.goikoetxea@hu-berlin.de
†josebainaki.juaristi@ehu.es
‡rdm@ehu.es
§wapalocm@ehu.es

[1] G. A. Somorjai, *Introduction to Surface Chemistry and Catalysis* (Wiley, New York, 1994).
[2] F. Bozso, G. Ertl, and M. Weiss, J. Catal. **50**, 519 (1977).
[3] M. Grunze, M. Golze, W. Hirschwald, H. J. Freund, H. Pulm, U. Seip, M. C. Tsai, G. Ertl, and J. Küppers, Phys. Rev. Lett. **53**, 850 (1984).
[4] L. J. Whitman, C. E. Bartosch, W. Ho, G. Strasser, and M. Grunze, Phys. Rev. Lett. **56**, 1984 (1986).
[5] C. T. Rettner and H. Stein, Phys. Rev. Lett. **59**, 2768 (1987).
[6] K. Homann, H. Kuhlenbeck, and H.-J. Freund, Surf. Sci. **327**, 216 (1995).
[7] S. Pick, P. Légaré, and C. Demangeat, Phys. Rev. B **75**, 195446 (2007).
[8] R. C. Egeberg, S. Dahl, A. Logadottir, J. H. Larsen, J. Nørskov, and I. Chorkendorff, Surf. Sci. **491**, 183 (2001).
[9] A. Logadottir and J. K. Nørskov, Surf. Sci. **489**, 135 (2001).
[10] S. Riikonen, A. S. Foster, A. V. Krasheninnikov, and R. M. Nieminen, Phys. Rev. B **80**, 155429 (2009).
[11] M. Gsell, P. Jakob, and D. Menzel, Science **280**, 717 (1998).
[12] M. Yata, Y. Uesugi-Saitow, M. Kitajima, A. Kubo, and V. E. Korsukov, Phys. Rev. Lett. **91**, 206103 (2003).
[13] M. Mavrikakis, B. Hammer, and J. K. Nørskov, Phys. Rev. Lett. **81**, 2819 (1998).
[14] A. Schlapka, M. Lischka, A. Groß, U. Kräsberger, and P. Jakob, Phys. Rev. Lett. **91**, 016101 (2003).
[15] S. Sakong and A. Groß, Surf. Sci. **525**, 107 (2003).
[16] J. R. Kitchin, J. K. Nørskov, M. A. Barteau, and J. G. Chen, Phys. Rev. Lett. **93**, 156801 (2004).
[17] G. Laurent, H. F. Busnengo, P. Rivière, and F. Martín, Phys. Rev. B **77**, 193408 (2008).
[18] G. Laurent, F. Martín, and H. F. Busnengo, Phys. Chem. Chem. Phys. **11**, 7303 (2009).
[19] L. A. Mancera, R. J. Behm, and A. Groß, Phys. Chem. Chem. Phys. **15**, 1497 (2013).
[20] M. Ramos, M. Minniti, C. Díaz, D. Farías, R. Miranda, F. Martín, A. E. Martínez, and H. F. Busnengo, Phys. Chem. Chem. Phys. **15**, 14936 (2013).
[21] H. F. Busnengo, A. Salin, and W. Dong, J. Chem. Phys. **112**, 7641 (2000).
[22] B. Hammer, L. B. Hansen, and J. K. Nørskov, Phys. Rev. B **59**, 7413 (1999).
[23] G. Kresse and J. Hafner, Phys. Rev. B **47**, 558 (1993).
[24] G. Kresse and J. Furthmüller, Comput. Mater. Sci. **6**, 15 (1996).
[25] O. Fruchart, P. O. Jubert, M. Eleoui, F. Cheynis, B. Borca, P. David, V. Santonacci, A. Lird, M. Hasegawa, and C. Meyer, J. Phys. Condens. Matter **19**, 053001 (2007).
[26] X. Qian and W. Hübner, Phys. Rev. B **60**, 16192 (1999).
[27] S. F. Huang, R. S. Chang, T. C. Leung, and C. T. Chan, Phys. Rev. B **72**, 075433 (2005).
[28] J. Łażewski, P. Piekarz, A. M. Oleś, J. Korecki, and K. Parlinski, Phys. Rev. B **76**, 205427 (2007).
[29] M. Albrecht, U. Gradmann, T. Reinert, and L. Fritsche, Solid State Commun. **78**, 671 (1991).
[30] I. Goikoetxea, M. Alducin, R. Díez Muiño, and J. I. Juaristi, Phys. Chem. Chem. Phys. **14**, 7471 (2012).
[31] The most significant change is that the effective energy barrier to dissociation obtained with adiabatic classical dynamics calculations from 50 000 trajectories is 1.5 instead of 1.6 eV.
[32] J. C. Tully, J. Chem. Phys. **73**, 1975 (1980).
[33] H. F. Busnengo, M. A. Di Césare, W. Dong, and A. Salin, Phys. Rev. B **72**, 125411 (2005).
[34] J. K. Vincent, R. A. Olsen, G.-J. Kroes, M. Luppi, and E.-J. Baerends, J. Chem. Phys. **122**, 044701 (2005).
[35] I. M. N. Groot, H. Ueta, M. J. T. C. van der Niet, A. W. Kleyn, and L. B. F. Juurlink, J. Chem. Phys. **127**, 244701 (2007).
[36] G. A. Bocan, R. D. Muiño, M. Alducin, H. F. Busnengo, and A. Salin, J. Chem. Phys. **128**, 154704 (2008).
[37] H. F. Busnengo and A. E. Martínez, J. Phys. Chem. C **112**, 5579 (2008).
[38] K. R. Geethalakshmi, J. I. Juaristi, R. Díez Muiño, and M. Alducin, Phys. Chem. Chem. Phys. **13**, 4357 (2011).
[39] J. P. Perdew, J. A. Chevary, S. H. Vosko, K. A. Jackson, M. R. Pederson, D. J. Singh, and C. Fiolhais, Phys. Rev. B **46**, 6671 (1992).
[40] R. van Harrevelt, K. Honkala, J. K. Nørskov, and U. Manthe, J. Chem. Phys. **122**, 234702 (2005).
[41] B. Hammer, M. Scheffler, K. W. Jacobsen, and J. K. Nørskov, Phys. Rev. Lett. **73**, 1400 (1994).
[42] P. Kratzer, B. Hammer, and J. K. Nørskov, Surf. Sci. **359**, 45 (1996).
[43] M. Gajdoš, J. Hafner, and A. Eichler, J. Phys. Condens. Matter **18**, 41 (2006).